研究成果の刊行に関する一覧表レイアウト（参考）

書籍

著者氏名	論文タイトル名	書籍全体の編集者名	書　籍　名	出版社名	出版地	出版年	ページ
なし							

雑誌

発表者氏名	論文タイトル名	発表誌名	巻号	ページ	出版年
Miura Y, Koyanagi Y	Death ligand-mediated apoptosis in HIV infection	Reviews in Medical Virology	in press		
Matsuura-Sawada R, Murakami T, Ozawa Y, Nabeshima H, Akahira J, Sato Y, Koyanagi Y, Ito M, Terada Y, Okamura K	Reproduction of menstrual changes in transplanted human endometrial tissue	Human Reproduction	in press		

雑誌

分担研究者氏名：岡本　尚

発表者氏名	論文タイトル名	発表雑誌名	巻号	ページ	出版年
Kobayashi, S., Kajino S., Takahashi, N., Kanazawa, S., Imai, K., Hibi, Y., Ohara, H., Itoh M. and Okamoto, T.	53BP2 induces apoptosis through the mitochondrial death pathway.	Genes Cells	in press		2005
Sanda, T., Iida, S., Ogura, H., Asamitsu, K., Murata, T., Bacon, K.B. Ueda R. and Okamoto, T.	Growth inhibition of multiple myeloma cells by a novel IkB kinase inhibitor.	Clin. Can. Res.	in press		2005
Tozawa, K., Okamoto, T., Kawai, N., Hashimoto, Y., Nagata, D., Hayashi, Y. and Kohri, K.	Positive correlation between sialyl Lewis X expression and pathological findings in renal cell carcinoma.	Kidney Int.	in press		2005
Okamoto,T.	The epigenetic alteration of synovial cell gene expression in rheumatoid arthritis and the roles of NF-kB and Notch signaling pathways.	Modern Rheum.	in press		2005
Tetsuka, T., Uranishi, H., Sanda, T., Asamitsu, K., Yang, J-P., Wong-Staal, F. and Okamoto, T.	RNA helicase A interacts with nuclear factor-[[kappa]]B p65 and functions as a transcriptional coactivator.	Eur. J. Biochem.	271	3741-3751	2004
Takahashi, N., Kobayashi, S., Jiang, X., Kitagori, K., Imai, K., Hibi, Y. and Okamoto, T.	Expression of 53BP2 and ASPP2 proteins from TP53BP2 gene by alternative splicing.	Biochem. Biophys. Res. Commun.	315	434-438	2004

書籍

分担研究者氏名：岡本　尚

著者名	題名	編集者名	書籍名	出版社名	出版地	出版年	ページ
岡本　尚	ウイルス性出血熱	山口　徹、北原光夫編	今日の治療指針２００４年版	医学書院	東京	2004	130-131
岡本　尚	新興・再興感染症の現状と今後	吉原なみ子	臨床病理レビュー特集号　流行感染症の脅威：最新情報とその対策	臨床病理刊行会	東京	2004	31-38
Okamoto, T.	Oxidative Stress in Rheumatoid Arthritis	Y-J. Surh and L. Packer	Oxidative Stress, Inflammation and Health	Marcel Dekker	USA	2005	in press

別紙５

研究成果の刊行に関する一覧表

書籍

著者氏名	論文タイトル名	書籍全体の編集者名	書籍名	出版社名	出版地	出版年	ページ

雑誌

発表者氏名	論文タイトル名	発表誌名	巻号	ページ	出版年
Shimizu,T., Arai,S., Imai,H., Oishi,T., Hirama,M., Koito,A., Kida,Y., & Kuwano,K	Glycoglycerolipid from the membranes of *Acholeplasma laidlawii* binds to human immunodeficiency virus type-1 (HIV-1) and accelerates its entry into cells.	Current Microbiol.	48,	182-188	2004

別紙 5

雑誌

発表者氏名	論文タイトル名	発表誌名	巻号	ページ	出版年
X. Zhou, M. Kubo, H. Nishitsuji, K. Kurihara, T. Ikeda, T. Ohashi, M Azuma, T. Masuda, and M. Kannagi.	Inducible co-stimulator (ICOS)-mediated suppression of human immunodeficiency virus type 1-replication in CD4+ T lymphocytes.	Virol.	325	252-263	2004
Y. Emori, T. Ikeda, T. Ohashi,T. Masuda, T. Kurimoto, M. Takei, and M. Kannagi.	Inhibition of human immunodeficiency virus type 1 replication by Z-100, an immunomodulator extracted from human type tubercle bacilli, in macrophages.	J. Gen. Virol.	85	2603-2613	2004
H. Nishitsuji, T. Ikeda, H. Miyoshi, T. Ohashi, M. Kannagi, and T. Masuda.	Expression of small hairpin RNA by lentiviral-based vector confers efficient and stable gene-suppression of HIV-1 on human cells including primary non-dividing cells.	Microbes and Infection	6	76-85	2004
T. Ikeda, H. Nishitsuji, X. Zhou, N. Nara, T. Ohashi, M. Kannagi, and T. Masuda.	Evaluation of the functional involvement of Human immunodeficiency virus type 1 Integrase in nuclear import of viral cDNA during acute infection.	J. Virol.	78	11563-11573	2004

別紙 5

研究成果の刊行に関する一覧表レイアウト

書籍

著者氏名	論文タイトル名	書籍全体の編集者名	書 籍 名	出版社名	出版地	出版年	ページ
M. Kubo, H. Nishitsuji, H. Liu, K. Kuriihara, T. Masuda, and M. Kannagi.	Suppression of HIV-1 replication by HIV-1-irrelevant CD8+ cytotoxic T lymphocytes and their culture supernatants.		XV International AIDS Conference	Medimond S.r.l.	India	2004	15-19

International Immunology, Vol. 16, No. 3, pp. 455–465
doi: 10.1093/intimm/dxh045

The point mutation of tyrosine 759 of the IL-6 family cytokine receptor gp130 synergizes with HTLV-1 *pX* in promoting rheumatoid arthritis-like arthritis

Katsuhiko Ishihara[1,3], Shin-ichiro Sawa[3], Hideto Ikushima[3], Seiichi Hirota[4], Toru Atsumi[2], Daisuke Kamimura[3], Sung-Joo Park[2], Masaaki Murakami[3], Yukihiko Kitamura[4], Yoichiro Iwakura[5] and Toshio Hirano[1–3]

[1]Laboratory of Developmental Immunology, Graduate School of Frontier Biosciences, Osaka University, Suita, Osaka, Japan
[2]Laboratory for Cytokine Signaling, RIKEN Research Center for Allergy and Immunology, Yokohama, Kanagawa, Japan
[3]Department of Molecular Oncology (C7), Osaka University Graduate School of Medicine, Suita, Osaka, Japan
[4]Department of Pathology (C2), Osaka University Graduate School of Medicine, Suita, Osaka, Japan
[5]Center for Experimental Medicine, Institute of Medical Science, University of Tokyo, Minato-ku, Tokyo, Japan

Keywords: autoimmune disease, knock-in mouse, rheumatoid arthritis, Tax

Abstract

Rheumatoid arthritis (RA) is a polygenic autoimmune disease. The autoimmunity develops from synergistic actions of genetic and environmental factors. We generated a double-mutant mouse by crossing two murine models of RA, a gp130 mutant knock-in mouse (*gp130$^{F759/F759}$*) and an HTLV-1 *pX* transgenic mouse (*pX*-Tg), in a C57BL/6 background, which is resistant to arthritis. The mice spontaneously developed severe arthritis with a much earlier onset than the *gp130$^{F759/F759}$* mice and with a much higher incidence than did the *pX*-Tg mice. The symptoms of *gp130$^{F759/F759}$* mice, including lymphoadenopathy, splenomegaly, hyper-γ-globulinemia, autoantibody production, increases in memory/activated T cells and granulocytes in the peripheral lymphoid organs, and a decrease in the class II MHC^{bright} CD11c^{+} population, were augmented in the double mutants. Marked reductions in incidence, severity and immunological abnormalities were seen in the triple mutant, *IL-6$^{-/-}$/gp130$^{F759/F759}$/pX*-Tg, indicating that the arthritis in the double mutant is IL-6 dependent. *gp130$^{F759/F759}$/pX*-Tg is a unique mouse model for RA.

Introduction

Rheumatoid arthritis (RA) is a systemic autoimmune disease characterized by the progressive chronic inflammation of multiple joints, which leads to their destruction, thus disabling the patients. The incidence of RA is ~1% worldwide, but its etiology is not yet known. Several characteristics of RA, such as hyper-γ-globulinemia, autoantibody production, genetic linkage with the HLA-DR locus, and infiltration of T cells and plasma cells into the synovium, have suggested that immunological disorders play crucial roles in the pathogenesis of this disease (1). RA is a polygenic disease, and is caused by immunological disorders that develop from the synergistic actions of genetic and environmental factors, such as bacterial or viral infections. Clinical and experimental studies have revealed the involvement of inflammatory cytokines, such as tumor necrosis factor (TNF)-α, IL-1, and IL-6 in the pathophysiology of RA (2). For example, TNF-α promotes the growth of synovial cells and blocking the TNF-α signal is an effective therapy (3).

IL-6 is a pleiotropic cytokine that regulates multiple biological functions, such as the development of the nervous and

Correspondence to: T. Hirano, Department of Molecular Oncology (C7), Osaka University Graduate School of Medicine, 2-2 Yamada-oka Suita, Osaka 565-0871, Japan. E-mail: hirano@molonc.med.osaka-u.ac.jp

Transmitting editor: H. Karasuyama

Received 29 October 2003, *accepted* 28 November 2003

hematopoietic systems, acute-phase responses, inflammation, and immune responses (4). A causative role for IL-6 in autoimmune disease was first recognized because of the observation that the autoimmune symptoms of patients with cardiac myxoma, such as hyper-γ-globulinemia and autoantibody production, disappeared with the surgical removal of the tumor which produced IL-6 (5). Furthermore, a high concentration of IL-6 was detected in the synovial fluid and serum of RA patients (6). Since then, clinical studies have provided more evidence supporting the involvement of IL-6 in the pathogenesis of autoimmune diseases (4,7). Studies using IL-6 knock-out mice revealed that IL-6 is involved in the severity and progress of experimentally induced arthritis (8–10). However, it was not known whether an abnormality in IL-6 family cytokine/gp130 receptor signaling was involved in spontaneous autoimmune diseases until we showed that a point mutation of the IL-6 family cytokine receptor, gp130, spontaneously caused RA-like autoimmune disease (11).

The IL-6 receptor consists of two molecules, the IL-6 receptor α chain and gp130, which is shared among the receptors for the IL-6 family cytokines. The ligand binding of gp130 activates two major signal-transduction pathways, the STAT3-mediated signal and the SHP-2/Gab/MAPK signal, in a manner dependent on the YXXQ motif and tyrosine (Y) 759 of gp130 respectively (12,13).

To clarify the roles played by the SHP-2- and STAT3-mediated signal-transduction pathways *in vivo*, we generated a series of knock-in mouse lines in which the gp130-mediated STAT3 or SHP-2 signals are selectively disrupted, by mutating the tyrosine residues of all the YXXQ motifs or Y759 to phenylalanine (*gp130$^{FXXQ/FXXQ}$* and *gp130$^{F759/F759}$* mice respectively). Our analysis of these mice indicated that the SHP-2-mediated or Y759-dependent signals negatively regulate the biological responses elicited by the STAT3-mediated signals *in vivo*, and that the balance of positive and negative signals generated through gp130 is skewed or shifted to positive STAT3 signaling in *gp130$^{F759/F759}$* mice (14). Importantly, the *gp130$^{F759/F759}$* mice spontaneously develop an RA-like autoimmune disease at ~1 year of age (11). *gp130$^{F759/F759}$* mice show severe immunological abnormalities, including autoantibody production, increased memory/activated T cells, impaired thymic negative selection and peripheral clonal deletion. Most importantly, the development of the RA-like disease is totally dependent on mature lymphocytes.

HTLV-1 is the causative agent of adult T cell leukemia. HTLV-1 encodes a transcriptional *trans*-activator, Tax, in the *env-pX* region, that *trans*-activates transcription from the cognate viral promoter (15,16). Tax also activates many cellular genes for cytokines, cytokine receptors and immediate early transcriptional factors (17–20). HTLV-I is also associated with several chronic inflammatory diseases, such as HTLV-1-associated myelopathy/tropical spastic paraparesis and HTLV-I-associated arthropathy (21). The HTLV-1 transgenic mouse is an animal model of arthritis that is triggered by viral infection (22). This mouse develops a form of arthritis resembling human RA, accompanied by increased gene expression of inflammatory cytokines including IL-6, MHC molecules in the joints and resistance of T cells to Fas-mediated apoptosis (23). The susceptibility to arthritis is dependent on the genetic background of the mice; BALB/c mice are susceptible, but C57BL/6 mice are resistant to arthritis (24).

Here, we report clear synergism between the point mutation of Y759 of gp130 and the HTLV-1 *pX* gene in the C57BL/6 genetic background, in which the HTLV-1 *pX* gene alone cannot induce RA-like joint disease. The double-mutant mouse *gp130$^{F759/F759}$/pX*-Tg developed severe arthritis much earlier than the *gp130$^{F759/F759}$* mouse. Lympho-hematopoietic abnormalities of the *gp130$^{F759/F759}$* mice, such as splenomegaly, lymphoadenopathy, hyper-γ-globulinemia, autoantibody production, and increased granulocytes and memory/activated T cells, were augmented in the *gp130$^{F759/F759}$/pX*-Tg mice. These abnormalities, as well as the onset, incidence and severity of the arthritis, were ameliorated in IL-6-deficient *gp130$^{F759/F759}$/pX*-Tg mice. The *gp130$^{F759/F759}$/pX*-Tg double-mutant mouse is a unique mouse model for the polygenic autoimmune disease RA.

Methods

Mice

gp130$^{F759/F759}$ knock-in mice that had been backcrossed to C57BL/6 5 times or more were mated with HTLV-1 *env-pX*-transgenic mice (*pX*-Tg) that had been backcrossed 17 times to C57BL/6 (B6). The litters of the F_1 generation were intercrossed to obtain *gp130$^{F759/F759}$/pX*-Tg double mutants. Thus the double mutants were thought as backcrossed 6 times to B6 (N6). In all the analyses including the studies of clinical course, we used the wild-type and single-mutant mice derived from the same littermates to generate the double- or triple-mutant mice.

IL-6-deficient mice were kindly given by Dr Kopf (25) and backcrossed 8 times to B6. They were then crossed with *gp130$^{F759/F759}$/pX*-Tg$^{+/-}$ to generate *IL-6$^{-/-}$gp130$^{F759/F759}$/pX*-Tg$^{+/-}$ triple mutants, which were equivalent to 7 times backcrossed to B6 (N7). All these mice were kept at the Institute of Experimental Animal Sciences at Osaka University Medical School.

Analyses of arthritis

Clinical assessment of arthritis. Mice were inspected every week for up to 24 weeks and assessed for signs of arthritis: redness, swelling and restriction of mobility. The severity of the arthritis (arthritis score) was based on the restriction of mobility, and swelling of the wrist and ankle joints, which were each examined bilaterally. The severity of the arthritis was graded on a scale of 0–4 as follows: 0 (no change), 1 (minimal change), 2 (mild change), 3 (moderate change) and 4 (severe change). The arthritis score shown is a sum of the scores assessed bilaterally to give a possible maximum of 16 points for each mouse. The incidence was defined as the percentage of mice with a score ≥2 points.

Radiologic and histologic analyses of arthritis. Radiologic and histologic data from B6 *gp130$^{F759/F759}$/pX*-Tg and 129/B6. *gp130$^{F759/F759}$* mice were obtained at 6–11 and 18 months of age respectively. X-ray photographs of the bones were taken using a Softex CMB-2 (Tokyo, Japan) and Fuji Film FR. For the histologic examination, joints were fixed in 10%

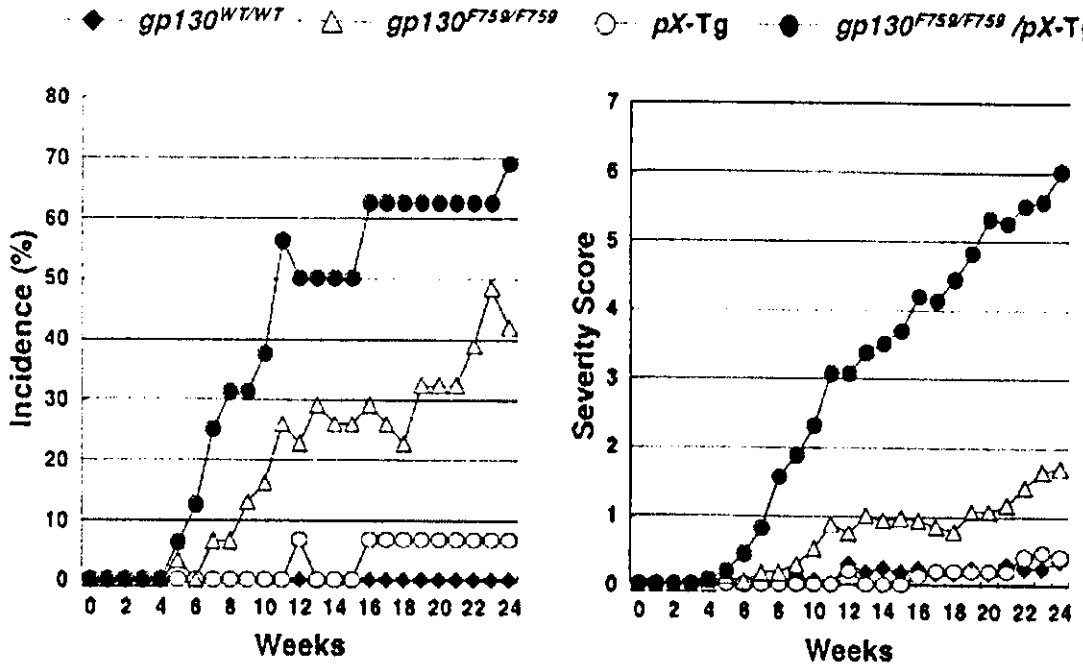

Fig. 1. Facilitated development and accelerated progress of arthritis in *gp130*$^{F759/F759}$/*pX*-Tg double-mutant mice. Double-mutant mice of the following genotypes were generated in the C57BL/6 background (N6) by crossing. *gp130*$^{WT/WT}$/*pX*-Tg$^{-/-}$ (black diamonds, n = 16; male 12, female 4), *gp130*$^{F759/F759}$/*pX*-Tg$^{-/-}$ (triangles, n = 31; male 14, female 17), *gp130*$^{WT/WT}$/*pX*-Tg$^{+/-}$ (white circles, n = 15; male 6, female 9) and *gp130*$^{F759/F759}$/*pX*-Tg$^{+/-}$ (black circles, n = 16; male 7, female 9). The severity of arthritis of each mouse was assessed weekly using the criteria described in Methods. Mice with scores ≥2 points were defined as arthritic. The incidence and average severity scores are indicated in the left and right graphs respectively.

formalin/neutral phosphate buffer, decalcified in 10% EDTA-4Na and embedded in paraffin. Sections were stained with hematoxylin & eosin.

Immunohistochemistry

Synovium of the knee joint was excised and frozen in OCT compound using liquid nitrogen. Serial sections were cut at a thickness of 5 μm and fixed with acetone. After inactivation of the endogenous peroxidase with 0.01% H_2O_2 in PBS, the sections were blocked with 5% goat serum in PBS and then incubated with rat or hamster mAb, or rabbit antibody. Bound rat mAb was detected with horseradish peroxidase (HRP)-labeled goat anti-rat IgG (Histofine; Nichirei, Japan) and visualized with 3,3′-diaminobenzidine (Dako, Kyoto, Japan). Bound hamster mAb and rabbit antibodies were detected using a biotinylated mouse anti-hamster mAb mixture (PharMingen, San Diego, CA) and biotinylated goat anti-rabbit IgG (Zymed, South San Francisco, CA) respectively. For class II MHC staining, a biotinylated mouse anti-class II MHC mAb (25-9-17; PharMingen) was used. Bound biotinylated antibodies were visualized with ABC for HRP (Vector, Burlingame, CA) and 3,3′-diaminobenzidine or ABC for alkaline phosphatase (Vector) and 5-bromo-4-chloro-3-indolyl phosphate/nitro-blue tetrazolium. For nuclear counterstaining, hematoxylin or methyl green was used in single- or dual-staining experiments respectively. The antibodies used were: rat anti-mouse IL-6 (MP5-20F; PharMingen), rat anti-CD4 (RM4-5; PharMingen), anti-CD11b (M1/70) and anti-granulocytes (Gr-1, RB6-8C5), hamster anti-CD3 mAb (48-2B; Santa-Cruz, CA), and rabbit anti-phospho-STAT3 (Tyr705) (Cell Signaling, Beverly. MA). Anti-CD11b and Gr-1 were purified from the culture supernatant of hybridomas in our laboratory.

Assay for serum antibodies and IL-6

Serum IgG concentrations were measured with an ELISA system as described previously (26). For the concentrations of serum autoantibodies and IL-6, commercially available ELISA systems for rheumatoid factor of the IgG class (Shibayagi, Shibukawa, Japan), anti-dsDNA antibody (Shibayagi) and IL-6 (Biosource, Camarillo, CA) were used.

Flow cytometry analysis

A single-cell suspension prepared from the spleen or lymph nodes by teasing the tissue with slide glass was stained with a combination of labeled mAb, and analyzed with a FACSCalibur and CellQuest software, as described previously (27). The mAb used were: FITC-conjugated Gr-1 (a marker for granulocytes), IM7 (anti-CD44; PharMingen), PC61 (CD25; PharMingen), AM/3 (IgM) and 25-9-17 (class II MHC, I-A^b; PharMingen), phycoerythrin (PE)-conjugated MEL14 (CD62L; Caltag, Burlingame, CA), H1.2F3 (CD69; PharMingen) and HL3 (CD11c; PharMingen), CyChrome-conjugated 53-6.7 (CD8; PharMingen) and RM4-5 (CD4; PharMingen), PECy5-conjugated Gr-1 (Southern Biotechnology Associates, Birmingham, Alabama), TriColor-conjugated RA3-6B2 (CD45R; Caltag), allophycocyanin-conjugated M1/70 (CD11b; PharMingen), CTCD4 (CD4; Caltag) and CTCD8 (CD8; Caltag), biotinylated CS/70 (IgD), and CyChrome-

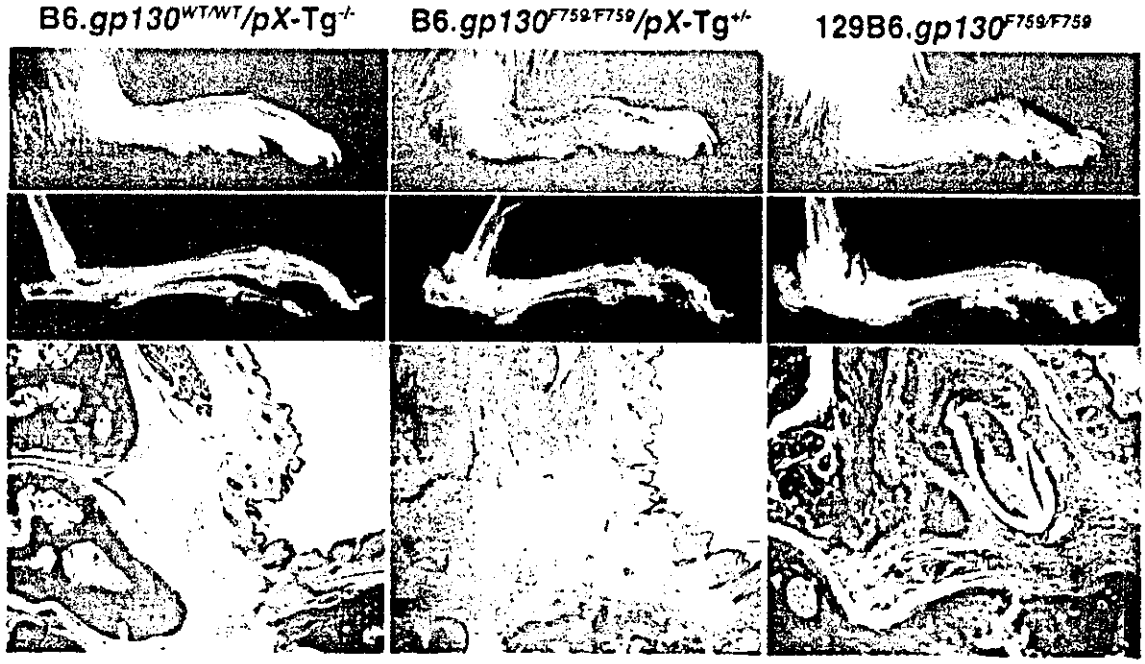

Fig. 2. Arthritis of $gp130^{F759/F759}$/*pX*-$Tg^{+/-}$. Macroscopic (top), radiologic (middle) and histologic (bottom) analyses of B6.$gp130^{WT/WT}$/*pX*-$Tg^{-/-}$ (left; 6 months old), B6.$gp130^{F759/F759}$/*pX*-$Tg^{+/-}$ (center; 6 months old) and 129/B6.$gp130^{F759/F759}$ (right; 18 months old) mice are shown. The histological analysis is of the synovium in the frontal portion of the ankles.

streptavidin (PharMingen). mAb Gr-1, AM/3 and CS/70 were purified from culture fluid supernatant and labeled with FITC or biotin by standard procedure.

Statistical analysis

Arthritis score, cell numbers of spleen and inguinal lymph nodes, ELISA assays, and frequencies of flow cytometry analyses of cell populations were compared by the Mann–Whitney *U*-test.

Results

Synergy between the Y759F mutation of gp130 and the HTLV-1 pX gene in the development of RA-like arthritis

pX-Tg mice in the C57BL/6 background (B6.*pX*-Tg mice) are resistant to arthritis (24). We generated double-mutant mice by crossing $gp130^{F759/F759}$ with B6.*pX*-Tg mice to determine the effects of *pX* gene expression with the $gp130^{F759/F759}$ mutation. The $gp130^{F759/F759}$/*pX*-Tg double mutants developed arthritis as young as 5 weeks old (Fig. 1). A 50% incidence of arthritis was observed at 11 weeks of age in B6.$gp130^{F759/F759}$/*pX*-Tg mice and within the 24-week observation period the incidence reached 70–100%. The incidences of male and female B6.$gp130^{F759/F759}$/*pX*-Tg mice at 24 weeks were 86 and 56% respectively. Only 7% of the B6.*pX*-Tg mice developed arthritis, with onset at ~16 weeks of age, consistent with the previous report that the C57BL/6 genetic background is resistant to the development of *pX*-dependent arthritis (24). Although the earliest symptom appeared in the B6 $g130^{F759/F759}$ mice at ~10 weeks of age, 50% incidence was observed at ~38 weeks of age (data not shown), indicating that the progress of arthritis in the $gp130^{F759/F759}$/*pX*-Tg double mutants was much faster than in the single mutants. The average severity score of the $gp130^{F759/F759}$/*pX*-Tg double mutants gradually increased to 6 points (male 7 points and female 5 points), while that of the $g130^{F759/F759}$ mice was <2 points within the 24-week observation period. These results indicate that the gp130 Y759F mutation and *pX* gene synergize in the development and progress of arthritis. This synergistic effect was also observed in the double mutants generated by mating with $g130^{F759/F759}$ mice backcrossed 8 times to B6, which generated the mutants with 9 times backcrossed to B6.

The earliest symptom of this arthritis was restriction of the movement of the wrist or ankle joints, which progressed to ankylosis with severe deformity of the wrists (not shown) and ankles (Fig. 2, top center). In radiologic analyses, the ankle joints of the B6.$gp130^{F759/F759}$/*pX*-Tg mice at 24 weeks of age (Fig 2, middle center) had erosions and deformity of bones, and ankylosis. Histological analysis of the $gp130^{F759/F759}$/*pX*-Tg mice at 24 weeks revealed hyperplasia of synovial fibroblasts, infiltration of neutrophils, narrowing of the joint spaces and ankylosis of the bone (Fig. 2, bottom center). These histological changes are similar to those observed in the arthritis of $gp130^{F759/F759}$ mice on the 129/B6 background at the age of 18 months (Fig. 2, right panels). Presence of the erosive arthritis and lack of nephropathy support this model to be RA-like rather than systemic lupus erythematosus-like, although both rheumatoid factor and anti-dsDNA antibody were detected in the sera.

To clarify the localization, interaction and activation status of the cells involved in this arthritis, we performed an immunohistochemical analysis of the synovium. Staining with

Fig. 3. Immunohistochemical analysis of the arthritic joints of *gp130$^{F759/F759}$/pX*-Tg$^{+/-}$ mice. Cryosections of the synovium of knee joints from a *gp130$^{F759/F759}$/pX*-Tg$^{+/-}$ mouse at 6 months old were stained with (A) hematoxylin & eosin, (B) anti-Gr-1 (brown), (C) anti-CD11b (brown; white arrow heads) and class II MHC (dark blue; black arrow heads), (D) anti-IL-6 (brown; arrow heads) and anti-TNFα (dark blue), (E) anti-CD4 (brown: a white arrow head) and anti-class II MHC (dark blue; a black arrow head), and (F) IL-6-producing cells (left; brown) and the nuclear localization of Y705 phosphorylated STAT3 (right; brown) in serial sections.

anti-CD11b (Fig. 3C) and anti-Gr-1 (Fig. 3B) mAb revealed that cells expressing CD11b or Gr-1 were mainly located in the layers of the synovial lining cells, indicating these were type A synovial cells. Co-localization of CD11b and Gr-1 was observed in the superficial lining cells, while the independent localizations of CD11b$^+$ or Gr-1$^+$ cells were observed in the sublining area, representing macrophages and granulocytes. There were areas containing scattered CD4$^+$ cells that overlapped with regions dominated by CD11b$^+$ cells in the sublining (Fig. 3C and E). Dual staining showed co-localization of CD3$^+$ cells with CD4$^+$ cells, confirming that most of the CD4$^+$ cells were T cells (not shown). Very few CD8$^+$ cells were observed (not shown). The area containing CD4$^+$ cells was closely located around or overlapping the area containing class II MHC$^+$ cells (Fig. 3E), suggesting this to be a location where certain immune responses take place. Class II MHC$^+$ cells overlapped with a portion of the CD11b$^+$ cells (Fig. 3C). Since CD11c$^+$ cells were rarely observed in the synovial sections (not shown), class II MHC$^+$CD11b$^+$ cells could be the main cell population presenting antigens in the synovium.

We then examined the production of inflammatory cytokines. An ELISA of serum IL-6 levels in *gp130$^{F759/F759}$/pX*-Tg mice aged 4–5 months old (101 ± 38 pg/ml; average ± SEM of $n = 9$) showed a 31 or 53% increase compared with *pX*-Tg (78 ± 32 pg/ml; $n = 7$) or *gp130$^{F759/F759}$* (66 ± 36 pg/ml; $n = 7$) mice respectively. Although these differences are not significant, it suggests that local IL-6 production is augmented in *gp130$^{F759/F759}$/pX*-Tg mice, probably due to the action of Tax, as reported previously (18). Immunohistochemically, local IL-6 production was observed at the superficial lining layers extending to the sublining areas in the arthritic synovium (Fig. 3D and F, left). The stronger staining at the sublining area and the shape of the cells indicate that synovial fibroblasts were the major IL-6 producers (Fig. 3F, left). IL-1β (not shown) and TNF-α (Fig. 3D) were faintly detected, but the staining was much weaker than that of IL-6, suggesting that IL-6 is the major inflammatory cytokine in this arthritis. To detect IL-6-mediated signaling, we examined the localization of phospho-STAT3. Some cells that were located in the area of IL-6 production also showed nuclear localization of phospho-STAT3 (Fig. 3F, right), suggesting that these cells were receiving aberrant gp130 signals from IL-6 produced at the site.

Synergy between the gp130 Y759F mutation and HTLV-1 pX for the generation of arthritis was dependent on IL-6.

Among the IL-6 family cytokine members that use gp130 as a signal-transducing receptor subunit, IL-6 plays a major role in the regulation of immune responses (28). Furthermore, the immunohistochemical analyses in the present study demonstrated that IL-6 was produced at the synovium in the arthritic joints and activated STAT3-mediated signaling. Thus, we examined the roles of IL-6 in the pathogenesis of the severe arthritis in *gp130$^{F759/F759}$/pX*-Tg double mutants by generating *IL-6$^{-/-}$/gp130$^{F759/F759}$/pX*-Tg triple mutants.

As shown in Fig. 4(A), arthritis in the *gp130$^{F759/F759}$/pX*-Tg double mutants started to appear in mice at 7 weeks old, whereas that of the *IL-6$^{-/-}$gp130$^{F759/F759}$/pX*-Tg triple mutants started in mice at 16 weeks old, 9 weeks later. The incidence of arthritis in the *IL-6$^{-/-}$gp130$^{F759/F759}$/pX*-Tg triple mutants then gradually increased, but at 24 weeks, when the incidence of arthritis in the *gp130$^{F759/F759}$/pX*-Tg double mutants had reached 100%, that in the *IL-6$^{-/-}$gp130$^{F759/F759}$/pX*-Tg triple mutants showed a plateau at 50%. Furthermore, the average severity score of the *IL-6$^{-/-}$gp130$^{F759/F759}$/pX*-Tg triple mutants was much lower than that of the *gp130$^{F759/F759}$/pX*-Tg double mutants (2 versus 6). These data indicated that IL-6 plays pivotal roles in determining the time of onset, final incidence and severity of the arthritis in the double mutants.

Histological examination revealed that hyperplasia of the synovial fibroblasts, infiltration of neutrophils and bone destruction were much ameliorated in the *IL-6$^{-/-}$gp130$^{F759/F759}$/pX*-Tg triple mutants (Fig. 4B, top). Radiologic analysis showed that the osteoporotic changes, erosive changes of the toes and reactive calcification of the tarsal bones seen in the *gp130$^{F759/F759}$/pX*-Tg mice were not observed in the *IL-6$^{-/-}$gp130$^{F759/F759}$/pX*-Tg triple mutants (Fig. 4B, bottom).

Immunological abnormalities caused by the synergy between the gp130Y759F mutation and HTLV-1 pX were dependent on IL-6

To clarify the role of IL-6 in the arthritis of *gp130$^{F759/F759}$/pX*-Tg double-mutant mice, various parameters of the lympho-

hematopoietic systems of each mouse were examined and compared. The average age of the mice in the groups analyzed was 32 weeks (range 24–40 weeks) and the genotypes and numbers of mice used were: *gp130*$^{WT/WT}$/*pX*-Tg$^{-/-}$ (n = 6), *gp130*$^{F759/F759}$/*pX*-Tg$^{-/-}$ (n = 5), *gp130*$^{WT/WT}$/*pX*-Tg$^{+/-}$ (n = 5), *gp130*$^{F759/F759}$/*pX*-Tg$^{+/-}$ (n = 8) and *IL-6*$^{-/-}$*gp130*$^{F759/F759}$/*pX*-Tg$^{+/-}$ (n = 5). The average severity score of *gp130*$^{F759/F759}$/*pX*-Tg (11.6 ± 1.2) was much higher than that of the arthritic mice *gp130*$^{F759/F759}$ (1.4 ± 0.9) and that of *IL-6*$^{-/-}$*gp130*$^{F759/F759}$/*pX*-Tg was significantly decreased (4.0 ± 1.6) (Fig. 5A).

Similar to the severity score, splenic cell number (Fig. 5B) and the titer of rheumatoid factor (Fig. 5E) of *gp130*$^{F759/F759}$/*pX*-Tg were significantly higher than those of wild-type or single mutants. The cell numbers of inguinal lymph node (Fig. 5C), and the concentrations of serum IgG (Fig. 5D) and anti-dsDNA antibody (Fig. 5F) showed increased values in the *gp130*$^{F759/F759}$ mouse group both in the presence or absence of *pX*

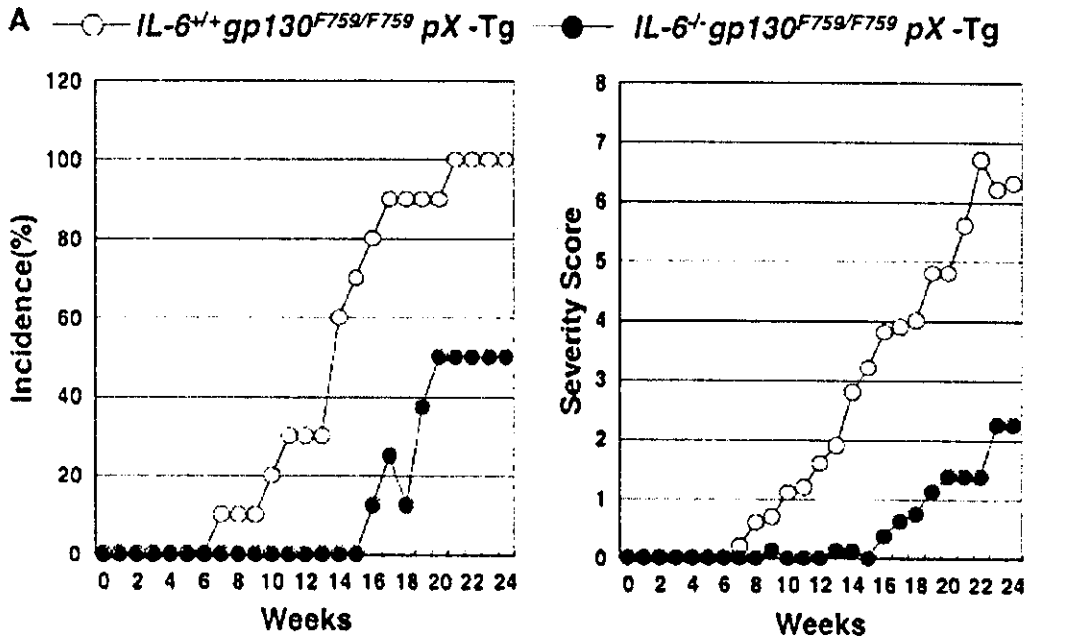

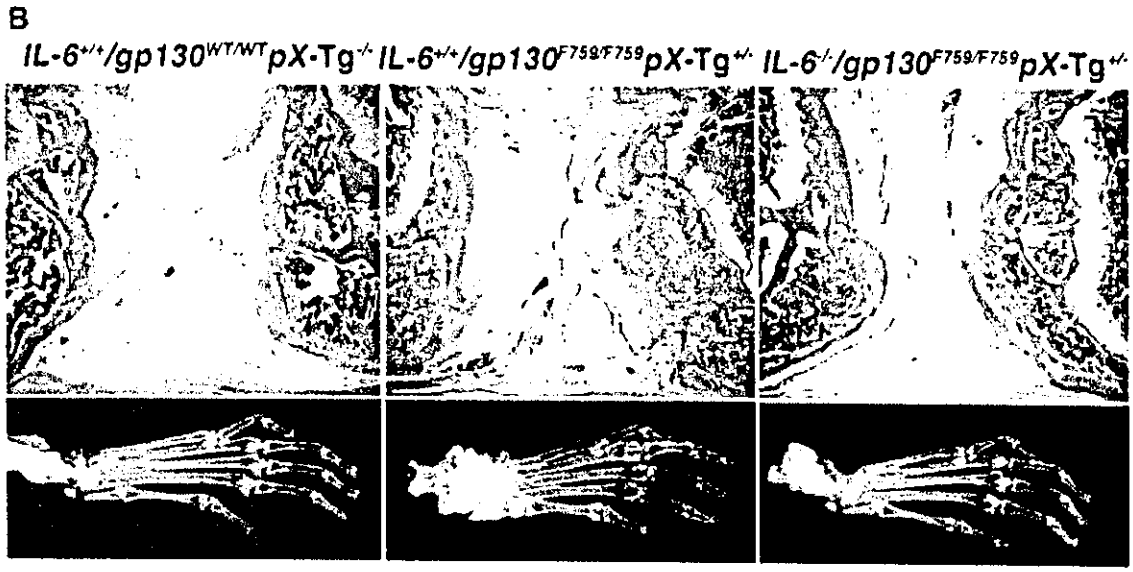

Fig. 4. IL-6 dependency of the arthritis in *gp130*$^{F759/F759}$/*pX*-Tg$^{+/-}$ mice. (A) Clinical course of arthritis in *gp130*$^{F759/F759}$/*pX*-Tg$^{+/-}$ (white circles, n = 10; male 6, female 4) and *IL-6*$^{-/-}$/*gp130*$^{F759/F759}$/*pX*-Tg$^{+/-}$ (black circles, n = 8; male 4, female 4) mice was examined. (B, top) Histologic analyses of the knee joint from 24-week-old *IL-6*$^{+/+}$/*gp130*$^{WT/WT}$/*pX*-Tg$^{-/-}$ (left), *IL-6*$^{+/+}$/*gp130*$^{F759/F759}$/*pX*-Tg$^{+/-}$ (center) and *IL-6*$^{-/-}$/*gp130*$^{F759/F759}$/*pX*-Tg$^{+/-}$ (right) mice. (B, bottom) Radiologic analyses of ankle joints arranged in the same order as in (B, top).

expression, indicating these changes are dependent on the *gp130*$^{F759/F759}$ mutation. These parameters, except for the inguinal lymph node cell numbers, normalized in the absence of IL-6, indicating significant IL-6 dependency.

Then we performed flow cytometry analyses to investigate the IL-6-dependent changes in the immune-competent cell populations of the inguinal lymph nodes (Fig. 6 and Table 1). Around 7 months old, only the reduction of naive CD4 T cells (CD62L$^+$CD44$^-$) and slight increases of activated CD4 T cells (CD62L$^+$CD44$^+$ or CD69$^+$) were observed in *gp130*$^{F759/F759}$ mice (Fig. 6A). In contrast, marked decreases of naive CD4 and CD8 T cells, and increases of memory/activated CD4$^+$ T cells (CD62L$^+$CD44$^+$, CD62L$^-$CD44$^+$ and CD69$^+$ cells), activated CD8$^+$ T cells (CD62L$^+$CD44$^+$ and CD69$^+$ cells) and granulocytes (CD11b$^+$Gr-1$^+$) were observed in *gp130*$^{F759/F759}$/*pX*-Tg, whereas these changes were almost normal in *IL-6*$^{-/-}$ *gp130*$^{F759/F759}$/*pX*-Tg$^{+/-}$ (Fig. 6A and B, and Table 1), suggesting that these changes are IL-6 dependent, and intimately related to autoimmunity and the severity of arthritis.

Since T cell activation is mainly regulated by professional antigen-presenting cells (29), we examined the dendritic cells in the lymph nodes of arthritic mice (Fig. 6B and Table 1). The average frequencies of CD11c$^+$ cells in the lymph nodes of wild-type and *gp130*$^{F759/F759}$/*pX*-Tg mice were 5 and 6%

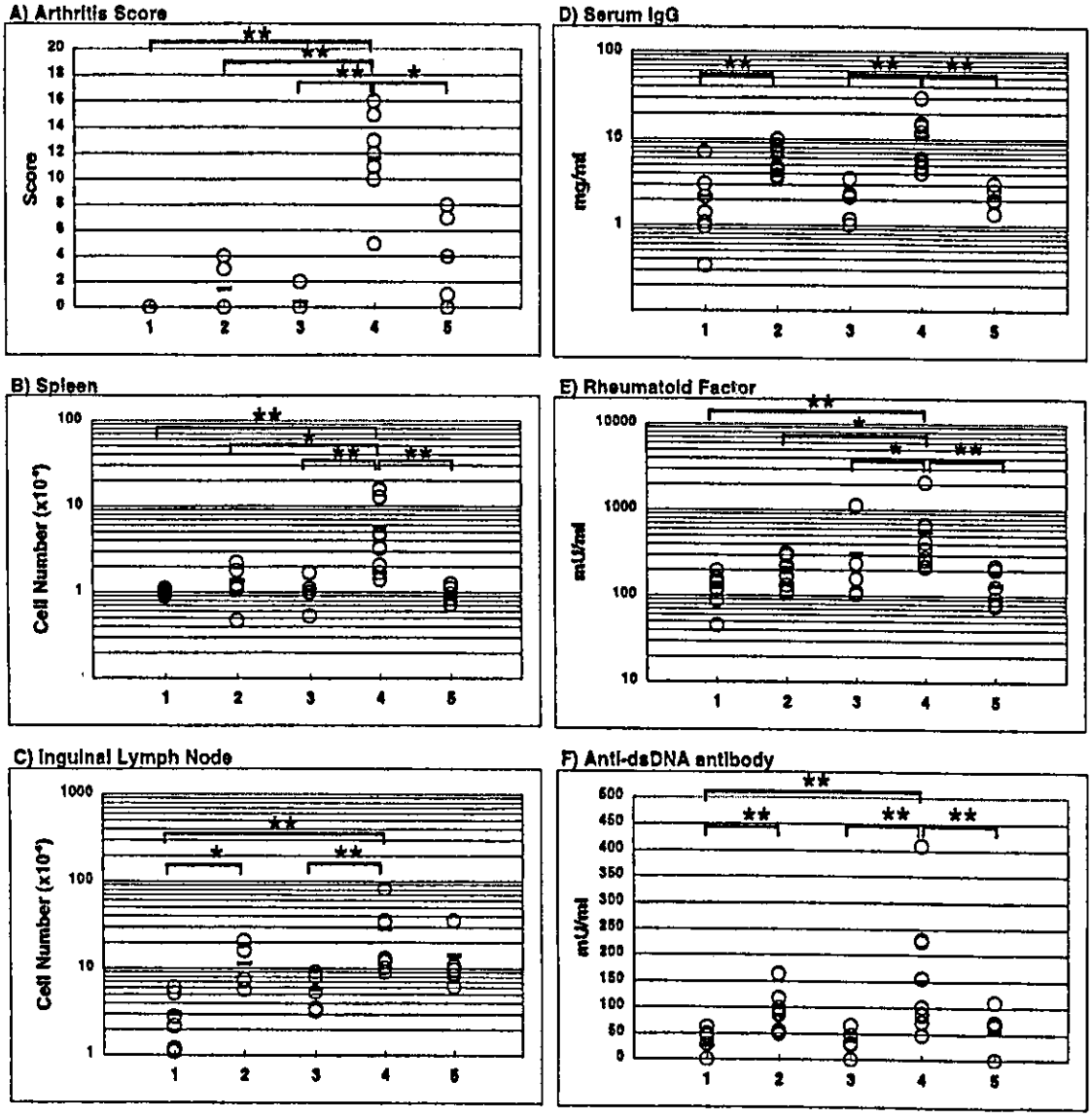

Fig. 5. IL-6 dependency of various parameters examined in the analysis of *gp130*$^{F759/F759}$/*pX*-Tg$^{+/-}$. The arthritis score (A), total cell number in the spleen (B) and bilateral inguinal lymph nodes (C), and concentrations of serum IgG (D), rheumatoid factor (E) and anti-dsDNA antibody (F) in mice averaging 32 weeks old (range 24–36) of the following genotypes are shown. The numbers on the horizontal axis indicate: 1, *gp130*$^{WT/WT}$/*pX*-Tg$^{-/-}$ (n = 6); 2, *gp130*$^{F759/F759}$/*pX*-Tg$^{-/-}$ (n = 5); 3, *gp130*$^{WT/WT}$/*pX*-Tg$^{+/-}$ (n = 5); 4, *gp130*$^{F759/F759}$/*pX*-Tg$^{+/-}$ (n = 8); and 5, *IL-6*$^{-/-}$/*gp130*$^{F759/F759}$/*pX*-Tg$^{+/-}$ (n = 5). The circles and horizontal bars indicate the values for each mouse and the average respectively. $^*P < 0.05$; $^{**}P < 0.01$

respectively, indicating that this double mutation did not greatly affect the development of dendritic cells. However, the expression levels of class II MHC (CIIMHC) molecules were drastically changed in the *gp130$^{F759/F759}$/pX*-Tg dendritic cells. Among CD11c^{+} cells, mature dendritic cells can be distinguished by the bright expression of class II MHC. In wild-type control mice, the CIIMHC^{bright} population represented 35% of the CD11c^{+} cells, whereas in *gp130$^{F759/F759}$/pX*-Tg mice it was only 4%. Furthermore, of the *IL-6$^{-/-}$gp130$^{F759/F759}$/pX*-Tg CD11c^{+} cells, the CIIMHC^{bright} population recovered to 29%, indicating that the decreased frequency of the CIIMHC^{bright} population was dependent on IL-6/gp130 signaling. A similar reduction of the CIIMHC^{bright} population was also observed in the CD11c^{+} cells of *gp130$^{F759/F759}$/pX*-Tg mice at 16 weeks of age, before the increase of memory or activated T cells was beginning to be obvious. Since this change of T cells follows a decreased frequency of CIIMHC^{bright}CD11c^{+} cells among lymph node cells, it may affect the regulation of T cell responses.

Discussion

We recently reported that a point mutation of gp130, a signal-transducing receptor subunit common to IL-6 family cytokines, causes RA-like autoimmune arthritis. This model, the *gp130$^{F759/F759}$* mouse, is unique and important because it provided the first experimental evidence that a point mutation of a cytokine receptor could cause autoimmune disease. Furthermore, the autoimmune disease spontaneously developed as a result of deregulated IL-6/gp130 signaling. In the *gp130$^{F759/F759}$* mouse, a point mutation of gp130 Y759F selectively disrupts the SHP-2-mediated gp130 signals, which results in the loss of ERK activation and in the prolonged activation of STAT3. Such unbalanced signaling is likely to be involved in triggering the breakdown of self-tolerance.

In this paper, we showed a clear synergy between the gp130 Y759F mutation and the HTLV-1 *pX* gene in causing RA-like arthritis, i.e. a genetic factor (the point mutation of gp130) and an environmental factor (the overexpression of *pX*, which mimics HTLV-1 infection) synergize, and facilitate the onset and progress of arthritis. It was surprising that the combination of a genetic factor for arthritis with late onset and slow progression, and a virus gene expression that evokes arthritis only rarely in a B6 genetic background, resulted in arthritis that had much earlier onset and faster progress than was seen in either single mutant. In the *gp130$^{F759/F759}$/pX*-Tg mouse, abnormalities previously observed in *gp130$^{F759/F759}$* mice were augmented. These include splenomegaly,

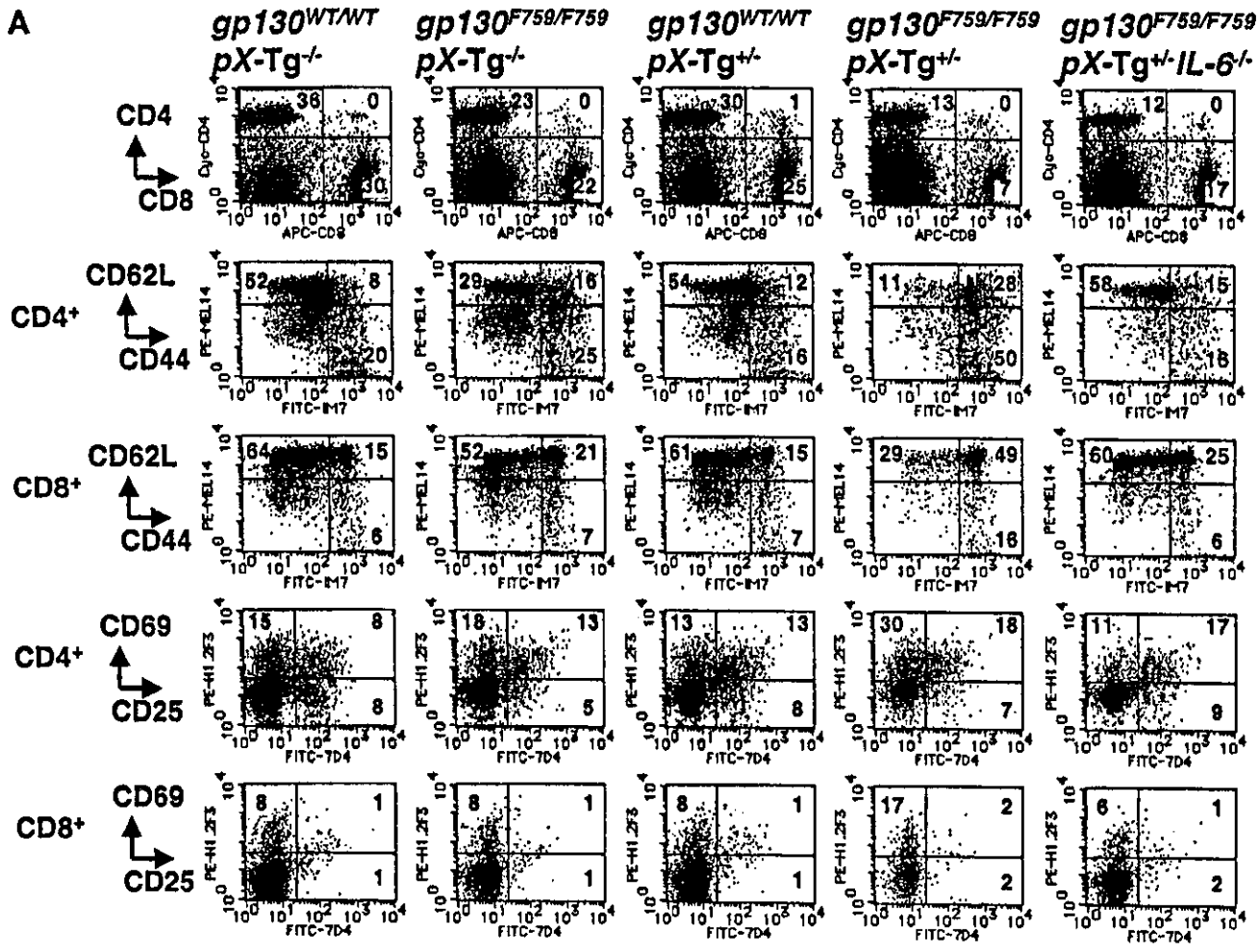

lymphoadenopathy, hyper-γ-globulinemia, autoantibody production, increases in granulocytes and memory/activated T cells, and decreases in naive T cells and class II MHC^{bright}CD11c^{+} cells. The clinical course of the triple mutant, *IL-6*$^{-/-}$*gp130*$^{F759/F759}$/*pX*-Tg, was markedly ameliorated, indicating that the acceleration of arthritis in *gp130*$^{F759/F759}$/*pX*-Tg is largely dependent on IL-6. Furthermore, almost all of the abnormalities seen in the *gp130*$^{F759/F759}$/*pX*-Tg mice were found to be dependent on IL-6, suggesting that these abnormalities are intimately related to the onset or progress of the disease.

Although we did not clarify the molecular mechanisms for the acceleration of the arthritis, we can speculate that the mutations in gp130 and the *pX* gene play distinct roles in this process. Since the latest analysis of arthritis in 8 times backcrossed B6.*gp130*$^{F759/F759}$ mice revealed that the incidence reached 100% at 54 weeks (unpublished observation), the major effect of the *pX* gene seems to be to accelerate the progression of the disease. The increased cytokine gene expression in *pX*-Tg reported previously supports this notion. In particular, IL-6 gene expression is known to be enhanced by *pX* and the synergy we observed was dependent on IL-6; therefore, it is likely that a *pX*-induced up-regulation of the IL-6 gene is one of the mechanisms. Since the major effect of *pX* expression is mediated by NF-κB activation, a role for *pX* could be as a substitute for TNF-α or IL-1 in virus-mediated effects.

On the other hand, because B6.*pX*-Tg rarely develops arthritis, the role of Y759F-mutated gp130 seems to be to trigger the disease in the *pX*-Tg mutant of an arthritis-resistant strain. Although IL-6 gene targeting in *gp130*$^{F759/F759}$/*pX*-Tg could not completely block the development of arthritis, the incidence reached a plateau at 50%, suggesting the involvement of other IL-6 family cytokines that utilize gp130.

Acknowledgements

This work is supported by a Grant-in-Aid for Scientific Research from the Ministry of Education, Culture, Sports, Science and Technology in Japan, and the Osaka Foundation for the Promotion of Clinical Immunology. We would like to thank Drs Y. Saeki and S. Ohshima for valuable advice and suggestions. We thank Ms R. Okuda for mouse maintenance, and Ms R. Sato for making cryo-sections and performing excellent technical assistance. We also thank Ms R. Masuda and A. Kubota for secretarial assistance.

Abbreviations

CII	class II
HRP	horseradish peroxidase
PE	phycoerythrin
RA	rheumatoid arthritis
Tg	transgenic
TNF	tumor necrosis factor

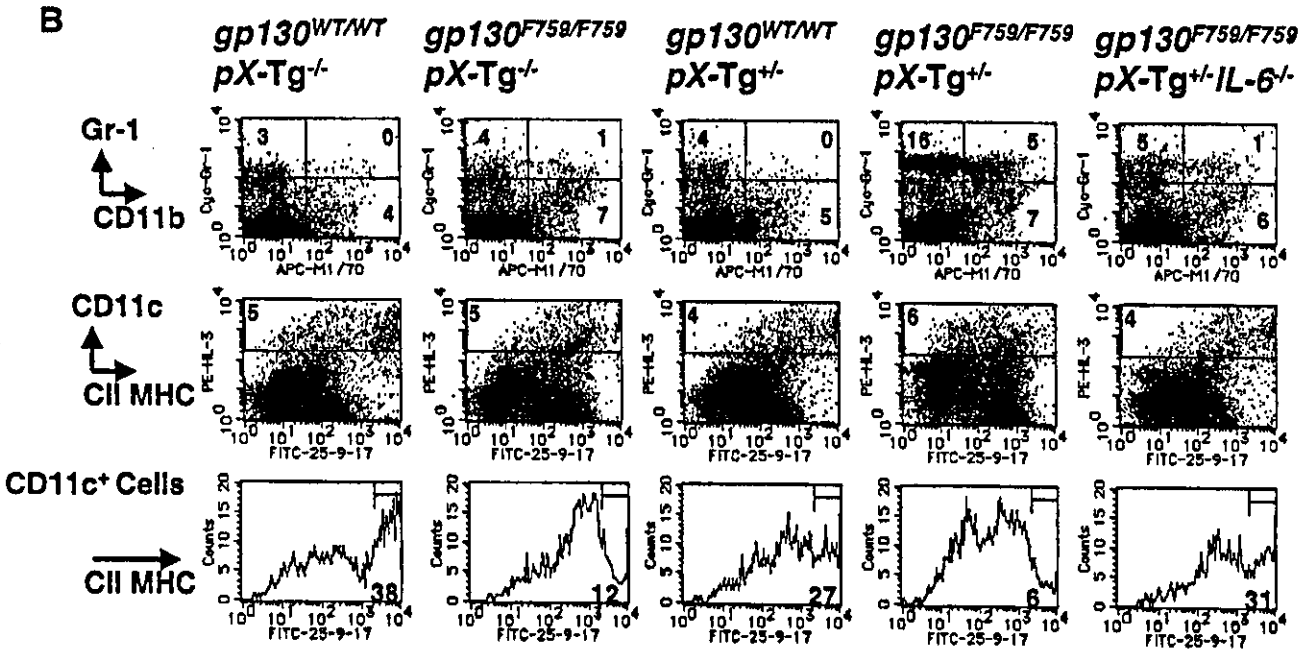

Fig. 6. IL-6-dependent changes of immune-competent cell populations in the inguinal lymph nodes of *gp130*$^{F759/F759}$/*pX*-Tg$^{+/-}$. The inguinal lymph node cells of each genotype at 7 months old were stained with the combination of mAb and analyzed with a flow cytometer as described in Methods. (A) Analyses of T cell subsets. (B) Analyses of myeloid cells. Numbers in the quadrants of dot-plots for CD4/CD8 and Gr-1/CD11b indicate the frequencies in total inguinal lymph node cells. Numbers in the quadrants of dot-plots for CD44/CD62L and CD25/CD69 indicate the frequencies in CD4^{+} or CD8^{+} inguinal lymph node cells. Numbers in the regions of dot-plots for CD11c/CIIMHC indicate the frequency of CD11c^{+} cells in the inguinal lymph node cells. In the histogram, the frequencies of CIIMHC^{bright} cells in the CD11c^{+} cells are indicated. Representative data from the analyses summarized in Table 1 are shown.

Table 1. Flow cytometry analysis of the lymph node cells of *gp130$^{F759/F759}$/pX*-Tg$^{+/-}$[a]

Cell type	*gp130/pX/IL-6*				
	W/W/W	*F/W/W*	*W/Tg/W*	*F/Tg/W*	*F/Tg/K*
CD4	30 ± 3	22 ± 2	**30 ± 1**[c]	**17 ± 2**	15 ± 1
CD62L$^+$CD44$^-$[b]	49 ± 6	38 ± 4	**54 ± 4**	**27 ± 7**	44 ± 8[d]
CD62L$^-$CD44$^+$	23 ± 4	25 ± 3	**16 ± 2**	**35 ± 7**	20 ± 2[d]
CD69$^+$CD25$^-$	11 ± 1	16 ± 2	11 ± 1	21 ± 2	12 ± 1[d]
CD8	25 ± 3	20 ± 2	**29 ± 2**	**14 ± 3**	19 ± 2
CD62L$^+$CD44$^-$	59 ± 3	53 ± 2	61 ± 3	39 ± 8	47 ± 7
CD62L$^+$CD44$^+$	**22 ± 3**	27 ± 3	25 ± 4	**39 ± 6**	26 ± 3[d]
CD69$^+$CD25$^-$	9 ± 1	11 ± 2	9 ± 1	17 ± 1	8 ± 1[d]
CD45R	40 ± 7	58 ± 6	**40 ± 4**	**50 ± 6**	55 ± 4
CD11b$^+$Gr-1$^-$	11 ± 2	8 ± 1	10 ± 3	11 ± 2	8 ± 2
CD11b$^+$Gr-1$^+$	0.5 ± 0.1	0.4 ± 0.1	0.4 ± 0.1	6.6 ± 4.0	0.6 ± 0.3[d]
CD11c$^+$	5 ± 1	NE	NE	6 ± 0	4 ± 0
CIIMHC^{bright}	35 ± 2	NE	NE	4 ± 1	29 ± 4[d]

[a]The inguinal lymph node cells of each genotype at 7 months old, as described in the Results and Fig. 5, were stained with the combination of mAb and analyzed with a flow cytometer as described in Methods. The abbreviations for the genotypes are: *W/W/W*, *F/W/W*, *W/Tg/W*, *F/Tg/W* and *F/Tg/K* for *gp130$^{WT/WT}$/pX*-Tg$^{-/-}$, *gp130$^{F759/F759}$/pX*-Tg$^{-/-}$, *gp130$^{WT/WT}$/pX*-Tg$^{+/-}$, *gp130$^{F759/F759}$/pX*-Tg$^{+/-}$ and *IL-6$^{-/-}$/gp130$^{F759/F759}$/pX*-Tg$^{+/-}$ respectively. Numbers indicate average frequencies ± SEM of each population in the inguinal lymph node cells except for those described in 'b'.

[b]The frequencies in the CD4$^+$ or CD8$^+$ inguinal lymph node cells are used for the cell populations defined by CD44/CD62L or CD25/CD69 expression, whereas the frequencies in the CD11c$^+$ cells are used for CIIMHC^{bright} CD11c$^+$ cells.

[c]Pairs of bold numbers in each population indicate that they are significantly different ($p < 0.05$).

[d]The frequencies returned to nearly normal in the absence of IL-6.

NE; not examined.

References

1 Firestein, G. S. 2003. Evolving concepts of rheumatoid arthritis. *Nature* 423:356.

2 Feldmann, M., Brennan, F. M. and Maini, R. N. 1996. Role of cytokines in rheumatoid arthritis. *Annu. Rev. Immunol.* 14:397.

3 Feldmann, M. and Maini, R. N. 2001. Anti-TNF alpha therapy of rheumatoid arthritis: what have we learned? *Annu. Rev. Immunol.* 19:163.

4 Hirano, T. 1998. Interleukin 6 and its receptor: ten years later. *Int. Rev. Immunol.* 16:249.

5 Hirano, T., Taga, T., Yasukawa, K., Nakajima, K., Nakano, N., Takatsuki, F., Shimizu, M., Murashima, A., Tsunasawa, S., Sakiyama, F., *et al.* 1987. Human B-cell differentiation factor defined by an anti-peptide antibody and its possible role in autoantibody production. *Proc. Natl Acad. Sci. USA* 84:228.

6 Hirano, T., Matsuda, T., Turner, M., Miyasaka, N., Buchan, G., Tang, B., Sato, K., Shimizu, M., Maini, R., Feldmann, M., *et al.* 1988. Excessive production of interleukin 6/B cell stimulatory factor-2 in rheumatoid arthritis. *Eur. J. Immunol.* 18:1797.

7 Ishihara, K. and Hirano, T. 2002. IL-6 in autoimmune disease and chronic inflammatory proliferative disease. *Cytokine Growth Factor Rev.* 13:357.

8 Alonzi, T., Fattori, E., Lazzaro, D., Costa, P., Probert, L., Kollias, G., De Benedetti, F., Poli, V. and Ciliberto, G. 1998. Interleukin 6 is required for the development of collagen-induced arthritis. *J. Exp. Med.* 187:461.

9 Ohshima, S., Saeki, Y., Mima, T., Sasai, M., Nishioka, K., Nomura, S., Kopf, M., Katada, Y., Tanaka, T., Suemura, M. and Kishimoto, T. 1998. Interleukin 6 plays a key role in the development of antigen-induced arthritis. *Proc. Natl Acad. Sci. USA* 95:8222.

10 Sasai, M., Saeki, Y., Ohshima, S., Nishioka, K., Mima, T., Tanaka, T., Katada, Y., Yoshizaki, K., Suemura, M. and Kishimoto, T. 1999. Delayed onset and reduced severity of collagen-induced arthritis in interleukin-6-deficient mice. *Arthritis Rheum.* 42:1635.

11 Atsumi, T., Ishihara, K., Kamimura, D., Ikushima, H., Ohtani, T., Hirota, S., Kobayashi, H., Park, S. J., Saeki, Y., Kitamura, Y. and Hirano, T. 2002 A point mutation of Tyr-759 in interleukin 6 family cytokine receptor subunit gp130 causes autoimmune arthritis. *J. Exp. Med.* 196:979.

12 Hirano, T., Ishihara, K. and Hibi, M. 2000. Roles of STAT3 in mediating the cell growth, differentiation and survival signals relayed through the IL-6 family of cytokine receptors. *Oncogene* 19:2548.

13 Kamimura, D., Ishihara, K. and Hirano, T. 2003. IL-6 signal transduction and its physiological roles: the signal orchestration model. *Rev. Physiol. Biochem. Pharmacol.* 149:1.

14 Ohtani, T., Ishihara, K., Atsumi, T., Nishida, K., Kaneko, Y., Miyata, T., Itoh, S., Narimatsu, M., Maeda, H., Fukada, T., Itoh, M., Okano, H., Hibi, M. and Hirano, T. 2000. Dissection of signaling cascades through gp130 *in vivo*: reciprocal roles for STAT3- and SHP2-mediated signals in immune responses. *Immunity* 12:95.

15 Sodroski, J. G., Rosen, C. A. and Haseltine, W. A. 1984. *Trans*-acting transcriptional activation of the long terminal repeat of human T lymphotropic viruses in infected cells. *Science* 225:381.

16 Fujisawa, J., Seiki, M., Sato, M. and Yoshida, M. 1986. A transcriptional enhancer sequence of HTLV-I is responsible for trans-activation mediated by p40 chi HTLV-I. *EMBO J.* 5:713.

17 Maruyama, M., Shibuya, H., Harada, H., Hatakeyama, M., Seiki, M., Fujita, T., Inoue, J., Yoshida, M. and Taniguchi, T. 1987. Evidence for aberrant activation of the interleukin-2 autocrine loop by HTLV-1-encoded p40x and T3/Ti complex triggering. *Cell* 48:343.

18 Muraoka, O., Kaisho, T., Tanabe, M. and Hirano, T. 1993. Transcriptional activation of the interleukin-6 gene by HTLV-1 p40tax through an NF-kappa B-like binding site. *Immunol. Lett.* 37:159.

19 Inoue, J., Seiki, M., Taniguchi, T., Tsuru, S. and Yoshida, M. 1986. Induction of interleukin 2 receptor gene expression by p40x encoded by human T-cell leukemia virus type 1. *EMBO J.* 5:2883.

20 Fujii, M., Niki, T., Mori, T., Matsuda, T., Matsui, M., Nomura, N. and Seiki, M. 1991. HTLV-1 Tax induces expression of various immediate early serum responsive genes. *Oncogene* 6:1023.

21 Kitajima, I., Yamamoto, K., Sato, K., Nakajima, Y., Nakajima, T., Maruyama, I., Osame, M. and Nishioka, K. 1991. Detection of human T cell lymphotropic virus type I proviral DNA and its gene

expression in synovial cells in chronic inflammatory arthropathy *J. Clin. Invest.* 88:1315.

22 Iwakura, Y., Tosu, M., Yoshida, E., Takiguchi, M., Sato, K., Kitajima, I., Nishioka, K., Yamamoto, K., Takeda, T., Hatanaka, M., *et al.* 1991. Induction of inflammatory arthropathy resembling rheumatoid arthritis in mice transgenic for HTLV-I. *Science* 253:1026.

23 Kishi, S., Saijyo, S., Arai, M., Karasawa, S., Ueda, S., Kannagi, M., Iwakura, Y., Fujii, M. and Yonehara, S. 1997. Resistance to fas-mediated apoptosis of peripheral T cells in human T lymphocyte virus type I (HTLV-I) transgenic mice with autoimmune arthropathy. *J. Exp. Med.* 186:57.

24 Iwakura, Y., Itagaki, K., Ishitsuka, C., Yamasaki, Y., Matsuzawa, A., Yonehara, S., Karasawa, S., Ueda, S. and Saijo, S. 1998. The development of autoimmune inflammatory arthropathy in mice transgenic for the human T cell leukemia virus type-1 env-pX region is not dependent on H-2 haplotypes and modified by the expression levels of Fas antigen. *J. Immunol.* 161:6592.

25 Kopf, M., Ramsay, A., Brombacher, F., Baumann, H., Freer, G., Galanos, C., Gutierrez-Ramos, J. C. and Kohler, G. 1995. Pleiotropic defects of IL-6-deficient mice including early hematopoiesis, T and B cell function, and acute phase responses. *Ann. NY Acad. Sci.* 762:308.

26 Itoh, M., Ishihara, K., Hiroi, T., Lee, B. O., Maeda, H., Iijima, H., Yanagita, M., Kiyono, H. and Hirano, T. 1998. Deletion of bone marrow stromal cell antigen-1 (CD157) gene impaired systemic thymus independent-2 antigen-induced IgG3 and mucosal TD antigen-elicited IgA responses. *J. Immunol.* 161:3974.

27 Ishihara, K., Kobune, Y., Okuyama, Y., Itoh, M., Lee, B. O., Muraoka, O. and Hirano, T. 1996. Stage-specific expression of mouse BST-1/BP-3 on the early B and T cell progenitors prior to gene rearrangement of antigen receptor. *Int. Immunol.* 8:1395.

28 Betz, U. A., Bloch, W., van den Broek, M., Yoshida, K., Taga, T., Kishimoto, T., Addicks, K., Rajewsky, K. and Muller, W. 1998. Postnatally induced inactivation of gp130 in mice results in neurological, cardiac, hematopoietic, immunological, hepatic, and pulmonary defects. *J. Exp. Med.* 188:1955.

29 Mellman, I. and Steinman, R. M. 2001. Dendritic cells: specialized and regulated antigen processing machines. *Cell* 106:255.

Journal of Medical Virology 74:328–335 (2004)

Secretory IgA Antibodies Provide Cross-Protection Against Infection With Different Strains of Influenza B Virus

Yasuko Asahi-Ozaki,[1]* Tomoki Yoshikawa,[1] Yoichiro Iwakura,[2] Yujiro Suzuki,[3] Shin-ichi Tamura,[1,4] Takeshi Kurata,[1] and Tetsutaro Sata[1]

[1]*Department of Pathology, National Institute of Infectious Diseases, Tokyo, Japan*
[2]*Center for Experimental Medicine, Institute of Medical Science, University of Tokyo, Tokyo, Japan*
[3]*Research Center for Biologicals, Kitasato Institute, Saitama, Japan*
[4]*Laboratory of Prevention of Viral Diseases (Research Foundation for Microbial Diseases of Osaka University), Research Institute for Microbial Diseases, Osaka University, Osaka, Japan*

This study examined whether secretory IgA (S-IgA) antibodies (Abs) could confer cross-protective immunity against infection with influenza B viruses of antigenically distinct lineages. Wild-type or polymeric Ig receptor (pIgR)-knockout (KO) mice were immunized by infection with different B viruses or by intranasal (i.n.) administration with different inactivated vaccines. Four weeks later mice were challenged with either the B/Ibaraki/2/85 virus, representative of the B/Victoria/2/87 (B/Victoria)-lineage, or B/Yamagata/16/88 virus, representative of the B/Yamagata-lineage. Three days after challenge, nasal wash and serum specimens were assayed for IgA and IgG Abs specific for challenge viral antigens and for protection against challenge viruses. In wild-type mice, B/Ibaraki (or B/Yamagata) cross-reactive IgA Abs were detected at higher levels when infected or immunized with homologous-lineage viruses and at lower levels when infected or immunized with heterologous-lineage viruses. There was a correlation between the amount of nasal cross-reactive IgA Ab and the efficacy of cross-protection with a homologous-lineage virus. In mice lacking the pIgR, nasal cross-protective IgA Abs were only marginally detected in vaccinated mice and an accumulation of IgA in the serum was observed. This reduction of nasal IgA was accompanied by inefficient cross-protection against the B/Ibaraki (or B/Yamagata) virus infection. These results suggest that challenge viral-antigen cross-reactive S-IgA in nasal secretions induced by i.n. infection or vaccination is involved in providing cross-protection against challenge infection with virus within either the B/Victoria- or B/Yamagata-lineage. ***J. Med. Virol. 74:328–335, 2004.*** © 2004 Wiley-Liss, Inc.

KEY WORDS: secretory IgA; cross-protection; Influenza B virus; pIgR-KO mice

INTRODUCTION

Influenza is a highly contagious and acute respiratory disease caused by influenza virus infection in the host respiratory tract (RT)-mucosa [Murphy and Webster, 1996]. Influenza A and B viruses usually cause annual world-wide epidemics and local outbreaks of influenza, respectively, by altering the antigenic properties of their surface hemagglutinin (HA) or neuraminidase (NA) to circumvent pre-existing host immunity [Hall et al., 1973; Housworth and Langmuir, 1974; Couch and Kasel, 1983; Murphy and Webster, 1996]. Two antigenically distinct lineages of influenza B virus, B/Victoria/2/87 (B/Victoria)-lineage and B/Yamagata/16/88 (B/Yamagata)-lineage, have been co-circulating in humans since 1988 [Kanegae et al., 1990; Kikuta et al., 1990; Rota et al., 1990].

Current inactivated vaccines administered subcutaneously induce systemic anti-viral IgG antibodies (Abs) that are highly protective against homologous virus infection but less effective against heterologous drifted virus infection [Couch and Kasel, 1983; Murphy and Webster, 1996]. However, many studies have shown that secretory IgA (S-IgA) induced by natural infection

*Correspondence to: Yasuko Asahi-Ozaki, PhD, Department of Pathology, National Institute of Infectious Diseases, 1-23-1 Toyama, Shinjuku-ku, Tokyo 162-8640, Japan.
E-mail: asahi@nih.go.jp

Accepted 14 June 2004
DOI 10.1002/jmv.20173
Published online in Wiley InterScience (www.interscience.wiley.com)

is more cross-protective against infection than serum IgG induced by parenteral vaccines in humans and in mice [Clements et al., 1983; Liew et al., 1984; Johnson et al., 1986; Murphy and Clements, 1989; Murphy, 1994; Renegar and Small, 1994]. In addition, S-IgA is primarily involved in protection against infection in the upper respiratory tract, whereas serum IgG diffuses into the lower respiratory tract where it provides protection [Ramphal et al., 1979; Liew et al., 1984; Kris et al., 1985]. It was shown that intranasal (i.n.) immunization of mice with a mixture of inactivated A virus vaccine and cholera toxin B subunits containing a trace amount of the holotoxin (CTB*) induced both S-IgA and serum IgG [Tamura et al., 1988, 1992a,b, 1994]. Studies on the control of influenza have involved primarily influenza A virus with relatively few studies involving influenza B virus [Liew et al., 1984; Tamura et al., 1988, 1992a,b, 1994; Kikuta et al., 1990; Mbawuike et al., 1999]. Since current vaccines include only a single strain of two lineages of B virus, one concern is that i.n. administration of adjuvant-combined inactivated vaccine could induce cross-protective mucosal immunity against not only drifted viruses of homologous-lineages but also viruses of heterologous-lineages.

The polymeric Ig receptor (pIgR), located on the basolateral side of mucosal epithelial cells, binds to dimeric IgA (dIgA) and transports it via a transcytotic vesicular network through the epithelial cells to the apical side. Finally, the pIgR is cleaved and dIgA is released into mucosal secretions in combination with the secretory component (SC) as S-IgA [Mostov and Deitcher, 1986; Brandtzaeg et al., 1994; Song et al., 1994; Tamer et al., 1995]. Recently, Shimada et al. [1999] established a mouse strain lacking exon 2 of the *pIgR* gene. pIgR-knockout (KO) mice have severely disrupted intestinal and hepatic transcytosis of dIgA which results in massive accumulation of dIgA in the serum. Using pIgR-KO mice to examine the cross-protective roles of S-IgA in influenza A virus infection, we found that actively secreted IgA plays an important role in cross-protection against variant A virus infections [Asahi et al., 2002]. However, it is not known whether S-IgA is also cross-protective under the same conditions for the two distinct lineages of influenza B virus infection.

In this study, we used wild-type mice infected previously with different B viruses or wild-type and pIgR-KO mice immunized i.n. with different CTB*-combined inactivated B virus vaccines to examine the roles of S-IgA in providing cross-protection against heterologous- and homologous-lineage B virus infection.

MATERIALS AND METHODS

Mice

pIgR-KO (pIgR −/−) mice were generated by intercrossing the N11 or N12 generation of homozygous mice from the offspring of heterozygous (pIgR +/−) mice which were kindly supplied by Yakult Central Institute for Microbiological Research (Tokyo, Japan) [Shimada et al., 1999, Asahi et al., 2002]. Wild-type BALB/c mice (female, 6–8 weeks old) were purchased from SLC (Hamamatsu, Japan).

Vaccines and Influenza Viruses

B/Ibaraki/2/85 (B/Ibaraki; passaged 10 times in mice and 3 times in eggs), B/Aichi/5/88 (B/Aichi; passaged 6 times in eggs), B/Nagasaki/1/87 (B/Nagasaki; passaged 5 times in eggs), B/Yamagata/16/88 (B/Yamagata; passaged 10 times in eggs), B/Mie/1/93 (B/Mie; passaged 8 times in eggs) were used. Influenza type A H1N1 strain (A/PR/8/34; A/PR8) was used as a control in some experiments. B/Yamagata and B/Mie were supplied by T. Odagiri (National Institute of Infectious Diseases, Tokyo, Japan). Viruses were propagated in the allantoic cavity of 10-day embryonated hen's eggs at 34°C for 48 hr and purified by centrifugation.

All vaccines used in this study were split-product virus vaccines prepared from the influenza virus isolates B/Ibaraki, B/Aichi, B/Nagasaki, B/Yamagata, B/Mie, and A/PR8, according to the method of Davenport et al. [1964] at the Kitasato Institute (Saitama, Japan). Briefly, each virus grown in the allantoic cavity of 10- to 11-day embryonated hen's eggs was concentrated, highly purified, and disrupted with ether. The vaccine contained whole proteins from the virus particle, with the major component being HA molecules (~30% of the total protein).

Immunization

Wild-type mice were anesthetized and immunized by dropping 1 μl of PBS containing mouse-adapted B/Ibaraki virus (5×10^4 $TCID_{50}$), B/Aichi (1.9×10^3 $TCID_{50}$), B/Nagasaki (1.9×10^3 $TCID_{50}$), B/Yamagata (2.7×10^4 $TCID_{50}$), B/Mie (1.3×10^4 $TCID_{50}$), or A/PR8 virus (1.9×10^3 $TCID_{50}$) into each nostril (2 μl per mouse). Similarly, wild-type and pIgR-KO mice were immunized by dropping 1 μl of PBS containing an inactivated vaccine into each nostril (5 μg viral protein/2 μl) together with CTB* [1 μg/2 μl CTB (Sigma-Aldrich, St. Louis, MO) supplemented with 0.2% cholera toxin (CT; Sigma-Aldrich)] under anesthesia [Tamura et al., 1992a; Tamura and Kurata, 1996].

Infection

Four weeks after immunization, the mice were challenged by dropping 1 μl of PBS containing a mouse-adapted B/Ibaraki virus (5×10^4 $TCID_{50}$) or B/Yamagata virus (2.7×10^4 $TCID_{50}$) into each nostril (2 μl per mouse) [Yetter et al., 1980; Tamura et al., 1996]. The nose-restricted volume (2 μl) of the virus suspension induced nose-localized infection that began in the nasal mucosa and spread to the lungs in 3–7 days, but was not lethal. The nasal wash virus titers, the peak of which was attained 3 days after infection, were used as indices of protection in the upper respiratory tracts of the immunized mice.

Specimens

Serum specimens were obtained from cardiac punctures of anesthetized mice and nasal wash specimens were collected by washing the nasal cavity of the excised head three times with a total of 1 ml of PBS containing 0.1% BSA [Tamura et al., 1992a; Asahi et al., 2002].

ELISA

The levels of IgA and IgG Abs against B/Ibaraki or B/Yamagata vaccine in the nasal wash and serum specimens were determined by ELISA as described previously [Tamura et al., 1992b]. Briefly, ELISA was carried out sequentially from the solid phase (EIA plate, Coster, Cambridge, MA) with a ladder of reagents consisting of: first, each vaccine; second, nasal wash or serum; third, goat anti-mouse IgA (α-chain specific; Kirkegaard & Perry Laboratories, Inc., Gaithersburg, MD) or goat anti-mouse IgG (γ-chain-specific; Jackson Immuno Research Lab Inc., West Grove, PA) conjugated with biotin; fourth, streptavidine conjugated with alkaline phosphatase (Life Technologies, Rockville, MD); and finally, *P*-nitrophenylphosphate. The amount of chromogen produced was measured by detecting absorbance at 405 nm with a Labsystems Multiskan MS autoreader (Thermo Electron, Inc., Helsinki, Finland). A standard for B/Ibaraki or B/Yamagata vaccine-reactive IgA or IgG (Ab) titration was prepared as follows. Pooled serum samples from either B/Ibaraki or B/Yamagata vaccine-immunized pIgR-KO or wild-type mice were purified using affinity columns conjugated with goat anti-mouse IgA (α-chain specific) or goat anti-mouse IgG (γ-chain-specific). The Ab titers of the purified IgA or IgG were measured by ELISA using 2-fold serial dilutions of each Ab and expressed as the highest sample dilution giving a positive reaction when the mean + 2 standard deviations (SD) of pre-immune sera was used as a cut-off value. The B/Ibaraki vaccine-reactive IgA or IgG, which had the same ELISA Ab titer (2^{12}), was used as a 320-unit standard after 100-fold dilution of the original purified IgA or IgG solution, and the B/Yamagata vaccine-reactive IgA or IgG, which had the same ELISA Ab titer (2^{10}), was used as a 80-unit standard after 100-fold dilution of the original IgA or IgG solution. The Ab titer of an unknown specimen was determined from the standard regression curve constructed by a 2-fold serial dilution of the standard for each assay.

Plaque Assays

The nasal wash virus titers peaked 3 days post-infection and were determined as previously described [Tobita, 1975; Tobita et al., 1975]. Briefly, serial 10-fold dilutions of the nasal washes were prepared, and 0.2-ml aliquots of each dilution were added to Madin-Darby canine kidney cells in a 6-well plate. After 1 hr of adsorption, each well was overlaid with 2 ml of agar medium. The plaques were counted after incubation for 48 hr in a CO_2 incubator. The virus titer was expressed in PFU per milliliter. The virus titer of each experimental group was represented by the mean ± SD of the virus titers per milliliter of specimens from five mice in each group.

Statistical Analyzes

Comparisons between experimental groups were performed by the Student's *t*-test. Values of $P < 0.05$ were considered significant unless otherwise indicated. Correlations between nasal IgA levels and nasal virus titers were determined by the Spearman's rank correlation coefficient.

RESULTS

Ab Responses and Protection Against Upper Respiratory Tract Infection by B/Ibaraki or B/Yamagata Viruses in Wild-Type Mice Infected Previously With Different B Viruses

B/Ibaraki or B/Yamagata vaccine-reactive IgA and IgG responses and protection against B/Ibaraki or B/Yamagata virus infection were examined in wild-type BALB/c mice previously infected with different B viruses. Five groups each containing five mice were infected i.n. with B/Victoria-lineage virus (B/Ibaraki, B/Aichi, or B/Nagasaki virus) or B/Yamagata-lineage virus (B/Yamagata or B/Mie virus). Four weeks after infection, mice were challenged by upper respiratory tract infection with B/Ibaraki or B/Yamagata virus. Three days post-challenge, nasal wash and serum specimens were collected to determine virus and Ab titers. As shown in Figure 1A, mice previously infected with B/Victoria-lineage had higher B/Ibaraki vaccine-reactive IgA and IgG responses and higher levels of protection against B/Ibaraki virus. Likewise, mice previously infected with B/Yamagata-lineage virus had higher B/Yamagata vaccine-reactive IgA and IgG responses and higher levels of protection against B/Yamagata virus (Fig. 1B). The efficacy of protection or cross-protection appeared to correlate with the increase in the nasal B/Ibaraki or B/Yamagata vaccine-reactive IgA titers, with a moderate inverse relationship between nasal virus shedding and nasal IgA titer ($r = -0.46$, $n = 70$). These results suggest that nasal B virus-reactive IgA Abs previously induced by natural B virus infection are involved in protection or cross-protection against re-infection with B virus, with specificity for either B/Victoria- or B/Yamagata-lineages.

Ab Responses and Protection Against Upper Respiratory Tract Infection by B/Ibaraki Viruses in Wild-Type and pIgR-KO Mice Immunized i.n. With Different Inactivated B Virus Vaccines

Protection or cross-protection against re-infection with B/Ibaraki viruses by nasal B/Ibaraki vaccine-reactive IgA Abs was higher in mice previously infected with B/Victoria-lineage viruses than in mice previously infected with B/Yamagata-lineage viruses (Fig. 1). To confirm the correlation between nasal IgA Abs and